J Exp Biol Advance Online Articles. First posted online on 2 September 2016 as doi:10.1242/jeb.140905
Access the most recent version at http://jeb.biologists.org/lookup/doi/10.1242/jeb.140905

Vision on the high seas: spatial resolution and optical sensitivity in two procellariiform seabirds with different foraging strategies

Mindaugas Mitkus*[,1], Gabrielle A. Nevitt [2], Johannis Danielsen [3], Almut Kelber [1]

[1] Lund Vision Group, Department of Biology, Lund University, Sölvegatan 35, 22364, Lund, Sweden

[2] Department of Neurobiology, Physiology and Behavior, College of Biological Sciences, University of California, Davis, One Shields Avenue, Davis, CA 95616, USA

[3] Department of Natural Sciences, University of the Faroe Islands, J. C. Svabos gøta 14, 100 Tórshavn, Faroe Islands

*Corresponding author: mindaugas.mitkus@biol.lu.se

Key-words bird visual ecology, retinal ganglion cell topography, visual spatial resolution, optical sensitivity, Leach's storm-petrel, Northern fulmar

Summary statement

We show that procellariiform seabirds with different nesting and foraging strategies also have evolved predictable differences in their ability to see their prey or other foraging seabirds.

Abstract

Procellariiform or ‘tubenosed’ seabirds are challenged to find prey and orient over the seemingly featureless oceans. Previous studies have found that life history strategy (burrow vs. surface nesting) was correlated to foraging strategy. Burrow nesters tended to track prey using dimethyl sulphide (DMS), a compound associated with phytoplankton, whereas surface-nesting species did not. Burrow nesters also tended to be smaller and more cryptic, whereas surface nesters were larger with contrasting plumage coloration. Together these results suggested that differences in life history strategy might also be linked to differences in visual adaptations. Here, we used Leach's storm-petrel, a DMS-responder, and Northern fulmar, a non-responder, as model species to test this hypothesis on their sensory ecology. From the retinal ganglion cell density and photoreceptor dimensions, we determined that Leach’s storm-petrels have six times lower spatial resolution than the Northern fulmars. However, the optical sensitivity of rod photoreceptors is similar between species. These results suggest that under similar atmospheric conditions Northern fulmars have six times the detection range for similarly sized objects. Both species have extended visual streaks with a central area of highest spatial resolution, but only the Northern fulmar has a central fovea. The prediction that burrow-nesting DMS responding procellariiforms should differ from non-responding species nesting in the open holds true for spatial resolution, but not for optical sensitivity. This result may reflect the fact that both species rely on olfaction for their nocturnal foraging activity, but that Northern fulmars might use vision more during daytime.

Journal of Experimental Biology • Advance article

Introduction

Petrels, albatrosses and shearwaters (order Procellariiformes) are adapted to forage over the oceans in search of ephemeral and patchily distributed prey. At small spatial scales (tens of square kilometres), they engage in an area-restricted search, using olfactory, visual or a combination of cues to find and capture their prey (Nevitt, 2008). While olfaction in procellariiforms has gained a lot of attention in recent years (reviewed by Nevitt, 2008), little is known about vision in procellariiforms.

One of the most studied olfactory info-chemicals in the marine environment is dimethyl sulphide (DMS) (Nevitt et al., 1995; Nevitt, 2011; Savoca and Nevitt, 2014). Some procellariiform species respond to experimental DMS deployments at sea by tracking it to the source (Nevitt et al., 1995). Behavioural trials performed under field laboratory conditions confirmed that some burrow-nesting species can detect DMS at pico-molar concentrations (Nevitt and Bonadonna, 2005). At the same time, other, primarily surface nesting species, do not show behavioural responses to it (Nevitt et al., 1995; Nevitt et al., 2004; Van Buskirk and Nevitt, 2008). As DMS can be associated with areas of high primary productivity, DMS-responsiveness is an adaptation for locating foraging hotspots by olfactory cues alone (Nevitt, 2011; Savoca and Nevitt, 2014).

Van Buskirk and Nevitt (2008) showed that DMS-responsiveness correlates to life history and that DMS responders also share certain morphological characteristics; they tend to be smaller, with cryptic coloration, whereas non-responders tend to be larger, less cryptically coloured, and adapted to exploit and effectively compete in large, mixed-species feeding aggregations. In experimental trials performed at sea, DMS responders also tended to be the "early detectors" of experimental prey patches and started to exploit them first, whereas DMS non-responders were preferentially attracted to odours of macerated krill (e.g., pyrazine). From these and other experiments, Nevitt et al. (2004) suggested that foraging activity elicited secondary olfactory cues (odours of macerated krill) and also visual cues (an increasing group size of various marine predators), which might attract "late detectors" - DMS non-responding species (Nevitt et al., 2004; Van Buskirk and Nevitt, 2008). Finally, they postulated that the lengthy developmental period spent in a dark burrow vs an open nest on the surface might have led them to evolve differences not only in their olfactory capabilities, but also in their visual performance.

To test this prediction, we performed comparative anatomical investigations of the visual systems of two sympatric species occurring in the Northern hemisphere that use these different foraging strategies - the burrow-nesting DMS responding Leach's storm-petrel (*Oceanodroma leucorhoa* Vieillot 1817) and the surface-nesting DMS non-responding Northern fulmar (*Fulmarus glacialis* Linnaeus 1761). The Leach's storm-petrel is one of the smallest procellariiforms (weight ca 38-54 g), and occurs in both the Atlantic and Pacific oceans. Depending on the foraging habitat, this

species feeds on crustaceans, fish, small cephalopods and soft-bodied invertebrates by surface-seizing, dipping or pattering (flying very slowly near the surface of the ocean with the feet touching the water) (Brooke, 2004). It is cryptically coloured, nests in burrows or crevices on rocky slopes, in grassland, or among trees and is strictly nocturnal at the colony (Brooke, 2004). The Northern fulmar is a medium size procellariiform (ca 600-800 g). This species feeds mostly on fish, crustaceans, cephalopods and carrion mainly by surface-seizing, but it can also perform short pursuit-plunges to depths of up to four meters. It nests in the open, usually on cliffs, and visits the nest during both day and night (Brooke, 2004).

Our aim was to compare and contrast visual performance in these two species that differ in foraging and life history characteristics. We focused our investigation on spatial resolution and sensitivity, the two key parameters of any optical system (Land and Nilsson, 2012). Spatial resolution, or visual acuity, describes the ability of an eye to resolve the details in a visual scene, and also provides an indication of the distance from which an animal can see objects. In the few bird species that have been investigated, optical quality of the eyes is excellent (Harmening et al., 2007; Maier et al., 2015), leaving only three factors that limit spatial resolution. First, the anterior focal length determines the size of the image reaching the photoreceptors in the retina; a large eye with a long focal length creates a larger image. Second, the density of the photoreceptor mosaic defines the amount of detail that can be captured from that image. Finally, the signals from photoreceptors converge onto retinal ganglion cells (RGCs); these are the neurons whose axons give rise to the optic nerve and send information to the visual centres of the brain. Because there are many fewer RGCs than photoreceptors, the convergence ratio tends to be less than 1:1 in most parts of the retina. Therefore species that need high visual acuity generally have large eyes with high photoreceptor and RGC densities (Hughes, 1977).

The RGC distribution in the retina is not uniform since there are areas of higher and lower cell density. Spatial resolution, therefore, cannot be equal across the visual field. The pattern of RGC density also varies between species, and it has been suggested that this variation is an adaptation to different habitat types ("terrain theory"; Hughes, 1977). For example, in an open terrain such as a savannah or the open ocean, all approaching objects are represented in a horizontal band on the retina (for a detailed explanation, see Hughes, 1977). Therefore, birds such as ostrich (*Struthio camelus*), little penguin (*Eudyptula minor*), king penguin (*Aptenodytes patagonicus*), and several species of owls (Strigiformes), waterfowl (Anseriformes: Anatidae) and procellariiform seabirds (Procellariiformes) procellariiforms have an elongated area of higher RGC density stretching across the retina called the visual streak (Hayes and Brooke 1990; Boire et al., 2001; Coimbra et al., 2012; Lisney et al., 2012a, 2013). This conformation of RGCs allows them to see fine details at the horizon without moving the head or eyes (Hughes, 1977). Species adapted to more cluttered

environments usually have a small circular area of higher visual acuity. This circular area, depending on its position in the retina, is called the area centralis or the area dorsalis and has been described in chickens (*Gallus gallus domesticus*), house sparrows (*Passer domesticus*), house finches (*Carpodacus mexicanus*), Carolina chickadees (*Poecile carolinensis*) and many other birds (Ehrlich, 1981; Dolan and Fernández-Juricic, 2010; Moore et al., 2013). Within retinal areas of high cell density, there might be a third retinal specialisation called the fovea (best known from the birds of prey). In the fovea, retinal neurons are centrifugally displaced creating a retinal indentation called a foveal pit. In contrast to the situation where there is an area centralis that lacks a pit, each RGC within the foveal pit sends the signal from only a single photoreceptor to the processing areas in the brain; this latter situation has been found in some raptor species (Oehme, 1964). However, in the fovea of some primate species, for example, the ratio of retinal ganglion cells to cones is greater than one (Wässle et al., 1990). Therefore, it has been suggested that, in species with a fovea, photoreceptor density determines spatial resolution; in species without a fovea, RGC density is a more reliable measure (Coimbra et al., 2015).

Along with spatial resolution, the second key parameter of any visual system is optical sensitivity, which determines visual performance in dim light. Optical sensitivity depends primarily on two factors: the 'brightness' of the retinal image and the dimensions of the photoreceptor cells (Land and Nilsson, 2012). The wider the pupil of an eye and the shorter the focal length, the brighter the image on the retina will be. The ratio of the focal length (*f*) and the entrance aperture diameter (*A*), the F-number (*f/A*), is often used in photography to describe the "brightness of the lens". At the level of the retina, wider and longer photoreceptors capture more light, and thus provide higher sensitivity. However, wider photoreceptors and shorter focal lengths result in lower spatial resolution. Therefore, there is a fundamental trade-off between high acuity and high sensitivity (Land and Nilsson, 2012). Birds that have highly acute vision, such as raptors, are not able to see well in very dim light, while birds that are adapted to see in very dim light, such as owls, tend to have low spatial resolution (Reymond, 1985; Harmening et al., 2009).

Given the differences in the life history and foraging strategies of the two procellariiform species we are investigating (Van Buskirk and Nevitt, 2008), we predict that the burrow-nesting, DMS-responsive Leach's storm-petrel should have lower visual acuity and increased optical sensitivity compared to the surface-nesting, DMS-non-responsive Northern fulmar. Since both species are adapted to forage pelagically, we also predict that both species will have a horizontal visual streak, as suggested by the "terrain theory" (Hughes, 1977).

Materials and methods

Study specimens

Leach's storm-petrels (*Oceanodroma leucorhoa* Vieillot 1817) were sampled at the breeding colony on Bon Portage Island, Nova Scotia, Canada, adjacent to a long-term, demographic study site (G. A. Nevitt, unpublished data). Pupil diameter was measured in six live breeding adult birds of unknown sex. For anatomical investigation, ten eyes from five individuals were taken. Birds were first anesthetized by an overdose of isoflurane and decapitated prior to dissection. We also included two additional eyes that were opportunistically collected from a freshly dead adult found on the edge of the colony.

Northern fulmars (*Fulmarus glacialis* Linnaeus 1761) were sampled during the breeding season in the Faroe Islands. Pupil diameter was measured in three live breeding adult birds of unknown sex during incubation. For anatomical analysis, thirteen eyes from ten adults were obtained opportunistically from birds shot for seabird pollution studies. Sample size and sampling methods were approved by the Canadian Wildlife Service (permit no. SC2767) and by the University of California Davis Institutional Animal Care and Use Committee (protocol no. 18084) for Leach's storm-petrels and by the Faroe Islands Museum of Natural History (permit no. 14/00066-15) for Northern fulmars.

Retinal wholemount preparation

Eyes from both species (Leach's storm-petrel: 3 birds, 6 eyes; Northern fulmar: 6 birds, 6 eyes) were enucleated in the field. The corneae and lenses were removed, and the remaining eyecups were fixed in 8% formaldehyde in phosphate buffered saline (PBS; 300 mOsm kg^{-1}, pH 7.3). Following fixation for 24 hours, eyes were transferred into PBS and stored until further processing in the laboratory.

Retinae were dissected and processed following standard methods (Stone, 1981, Mitkus et al., 2014). Briefly, eyes were washed in PBS, sclera and choroid were removed and remnants of pigment epithelium were bleached in a solution of 12% hydrogen peroxide in PBS at room temperature for 24 hours. After bleaching, the retinae were washed in PBS, flattened on gelatinized slides, and immersed in a bath with a mixture of formalin and absolute alcohol (1:25) for 24 hours to increase adherence to the slide (Stone, 1981). Retinal wholemounts were then rehydrated in a descending ethanol series, stained with an aqueous solution of 0.1% Cresyl Violet acidified with acetate buffer (pH 3.7), dehydrated in an ascending ethanol series, cleared in xylene, and cover-slipped using 'Cytoseal^{TM}XYL' (Richard-Allan Scientific) mounting medium. Pictures of the freshly mounted and stained retinae were taken to measure retinal dimensions and to evaluate retinal shrinkage during the staining procedure. The shrinkage was 18.0 ± 9.6% (mean ± s.d.) for

the Leach's storm-petrel and 6.2 ± 2.7% for the Northern fulmar retinae respectively. Final RGC densities were corrected for the shrinkage specific for each specimen.

Counting, measuring and mapping retinal cells in wholemount preparations

Cresyl Violet-stained cells were counted using a Nikon DS-Fi1c digital camera mounted on a Zeiss Axiophot microscope with a Plan-Neofluar 40x/1.30 Oil and a Plan-Apochromat 63x/1.40 Oil DIC objectives. The live-view mode of the N-Dis Elements software (Nikon) allowed us to mark cells as we counted them directly on the PC screen, thus avoiding double counting of the same cells. The counting frames (100 × 100 µm) were randomly and systematically placed within a grid of 0.5 × 0.5 mm in the high-density areas (that were well demarcated by differential intensity of staining) and 1 × 1 mm in the remaining retina of the Leach's storm-petrel. In the Northern fulmar retinae, counting frames (100 × 100 µm) were placed within a grid of 1 × 1 mm in the high-density areas and 2 × 2 mm in the remaining retina; nine additional counting frames were placed on the slopes of the fovea. All cells enclosed within the counting frame and those intersecting the acceptance lines, but not touching the rejection lines were included in the counts (Gundersen, 1977).

We did not differentiate between RGCs and displaced amacrine cells, because it has been previously shown that inclusion of displaced amacrine cells does not alter retinal topography or result in a substantial overestimation of the spatial resolving power in several species from different vertebrate taxa (Collin and Pettigrew, 1988; Pettigrew et al., 1988; Chen and Naito, 1999; Mitkus et al., 2014). However, we distinguished glial cells according to the criteria established by Ehrlich (1981), and excluded them from the final cell counts. Thus, wherever retinal ganglion cells (RGCs) are mentioned below, we are including neuronal cells (RGCs + displaced amacrine cells). Ganglion cell isodensity contour maps were created in MATLAB (R2012b, The MathWorks, Natick, MA, USA) using the biharmonic spline interpolation method without data smoothing, superimposed on the retinal wholemount contour lines and finalised in Adobe Illustrator CS6 (Adobe Systems Incorporated).

Retinal cross-section preparation and photoreceptor dimensions

Posterior parts of the eyeballs (N=2 Leach's storm-petrel, N=2 Northern fulmar) were dissected in the field and fixed in 2.5% glutaraldehyde in 0.1 M sodium cacodylate buffer. Following fixation for ~24 hours, eyes were transferred into buffer and stored until further processing in the laboratory. To examine photoreceptor morphology, pieces of central retina were cut out and rinsed several times in buffer. Following dehydration in an ascending ethanol series, the retinal pieces were incubated in a 2:1 mix of acetone and Epon for 30 minutes, 1:1 mix of acetone and Epon for 12 hours, and pure Epon for another 6 hours. The retinal pieces were then transferred into fresh Epon and polymerised for 48 hours at 60° C.

Thin sections (2 µm) were stained with 1% Toluidin Blue - 1% Borax, and cover-slipped using 'Cytoseal^{TM}XYL' (Richard-Allan Scientific) mounting medium. Photoreceptor dimensions were measured using the public domain software ImageJ 1.43u (Rasband, 1997-2012), using the same microscope as described above. Retinal shrinkage of the sections was evaluated by comparing oil droplet diameters in the processed Northern fulmar tissue to those of the fresh retina. Because fresh retina of Leach's storm-petrel was not available for evaluation, we assumed the same level of shrinkage (10%) as found in the Northern fulmar retinal sections. The oil droplet diameter was adjusted accordingly for both species.

Data for schematic eyes

To estimate the anterior focal length (also called the posterior nodal distance, *PND*) of the eye, we used Gullstrand's simplified schematic eye model as previously elaborated by Lind and Kelber (2009). We assumed emmetropic eyes (with distant light source focused on the retina) and set the refractive indices of the aqueous and vitreous humours to 1.337 (Martin and Brooke, 1991). To obtain mean parameters of the optical system for the model calculations, three eyes from three individuals of Leach's storm-petrel and five eyes from four individuals of the Northern fulmar were used. Fresh eyes left intact in the skulls, were quickly frozen in liquid nitrogen and sectioned horizontally (still intact in the skulls; Fig. 1A, C) using a cryostat (Microm HM 560). Photographs of the eye cross-sections and a micron scale were taken at intervals of 150 µm, and eye dimensions were measured using the public domain software ImageJ 1.43u (Rasband, 1997-2012).

To measure the maximum entrance pupil diameter for the eyes of Leach's storm-petrel, six birds were dark adapted to the light level of 0.0001 cd m^{-2} for two hours. Birds were filmed with an infrared (IR) camcorder (Sony HDR-XR500) with a ruler placed at the plane of the cornea. Three Northern fulmars were filmed with an IR camcorder (Sony LL 20) on their nests, and the dimensions of their beaks were used as a reference scale. For the Northern fulmars, we only analysed footage taken at least 1.5 hours after or before the start of civil twilight. Because the bill measurements of the individuals in the footage were not available, we used average bill depth at gonys of females (16.2±0.5 mm, mean±s.d; n=100) of the Northern fulmars from the Faroe Islands (J. Danielsen, unpublished data). Bill depth at gonys is smaller in females than males; therefore, actual pupil diameters might be larger if any of the individuals investigated was a male. For each individual of both species, five frames were extracted from footage that showed the bird looking directly into the camcorder (Fig. 1B, D), and maximum pupil diameter was measured using the public domain software ImageJ 1.43u (Rasband, 1997-2012).

Estimation of anatomical spatial resolving power

The spatial resolution limit for an achromatic grating was estimated based on both the RGC and cone peak densities. As RGCs are the only cells that connect the retina to the visual centres of the

brain, it is often assumed that the peak density of RGCs determines the theoretical upper limit of spatial resolution (Pettigrew et al., 1988; Lisney et al., 2012b). However, in a primate fovea, there are three to four midget RGCs connected to each photoreceptor (Wässle et al., 1990). Therefore, determining spatial resolution based on RGC density in the primate fovea would result in an overestimation. Moreover, in the fovea, RGCs are usually centrifugally displaced from the centre, meaning that the photoreceptors to which they connect are not in the same retinal column. Depending on how far and how asymmetrically the RGCs are displaced, this can cause incorrect spatial resolution estimates.

Whether a midget-like system exists in any avian species is currently unknown; however, Oehme (1964) has traced RGC to photoreceptor connections in the central and temporal foveae of a common buzzard (*Buteo buteo*) and a common kestrel (*Falco tinnunculus*), and has found one RGC for each foveal cone. Furthermore, Reymond (1985, 1987) has shown that the theoretical spatial resolution based on the peak cone density in the fovea of both a brown falcon (*Falco berigora*) and a wedge-tailed eagle (*Aquila audax*) closely matches behavioural visual acuity. However, Mitkus et al. (2014) have shown that in two afoveate parrot species (budgerigars (*Melopsittacus undulatus*) and Bourke's parrots (*Neopsephotus bourkii*)) spatial resolution based on peak cone density overestimates behavioural visual acuity. Because the determination of maximum spatial resolution will differ depending on whether or not a fovea is present, we measured both ganglion cell and cone density in each species. Where a fovea is absent, ganglion cell density is considered to provide the most accurate anatomical determination of spatial resolution whereas photoreceptor density in the foveal region is more accurate where there is a fovea (Coimbra et al., 2015).

Our underlying assumptions were that there are no rods in high-acuity regions (Coimbra et al., 2015), and that all types of cones and ganglion cells in high acuity regions contribute equally to high acuity tasks. Therefore, the anatomical spatial resolving power should be considered as a theoretical upper limit (Pettigrew et al., 1988). We then calculated the Nyquist limit of spatial resolution, F_{ng}, for a two-dimensional hexagonal array of cells, by the formula:

$$F_{ng} = \frac{\pi \times PND}{360} \times \sqrt{\frac{2D}{\sqrt{3}}}, \quad (1)$$

where *PND* is the posterior nodal distance, *D* is the peak ganglion cell density in cells mm^{-2}, and resolution is expressed in cycles per degree (cyc deg^{-1}) (Williams and Coletta, 1987).

We could not determine photoreceptor density in the high-acuity regions of the wholemounted retinae. Therefore, in order to estimate spatial resolution based on the peak photoreceptor density, we used the diameter of the cone oil droplet as the effective aperture of the cone (Stavenga and Wilts, 2014) and assumed hexagonal cell packing, which allows for the highest photoreceptor density, and thus the smallest receptor centre-to-centre distance (Snyder and Miller, 1977). Kram et

al. (2010) found almost perfect hexagonal packing even in the mid-peripheral retina of the domestic chicken, and showed that oil droplet diameters closely approximate receptor centre-to-centre distance.

We used the average oil droplet diameter measured in retinal cross-sections from the area centralis of the Leach's storm-petrel and from the central fovea of the Northern fulmar, and calculated spatial resolution F_{nc} by the following equation (Snyder and Miller, 1977):

$$F_{nc} = \frac{PND}{d\sqrt{3}}, \quad (2)$$

where *PND* is the posterior nodal distance, *d* is the oil droplet diameter and resolution is expressed in cyc deg^{-1}.

We calculated width of the minimum object d_{obj} to be seen at a given distance *L* with a given spatial resolution *F*, by:

$$d_{obj} = L \times \tan MAR, \quad (3)$$

where *MAR* is a Minimum Angle of Resolution. *MAR* is the angular size of the smallest detail that can be resolved by an eye. Per definition, this is equal to half the angular size of one cycle and can be expressed as:

$$MAR = \frac{1}{2F} \quad (4)$$

Optical sensitivity

We calculated the optical sensitivity (*S*) of single rod photoreceptors to white light as described by Warrant and Nilsson (1998):

$$S = (\frac{\pi}{4})^2 \times A^2 \times (\frac{a}{PND})^2 \times (\frac{k \times l}{2.3 + k \times l}), \quad (5)$$

where *A* is the pupil diameter, *a* is the diameter of the photoreceptor outer segment, *PND* is the posterior nodal distance, *k* is the absorption coefficient of the photoreceptor (*k*=0.053 μm^{-1}; Warrant and Nilsson, 1998), and *l* is the length of the photoreceptor outer segment.

Results

Retinal morphology and ganglion cell topography

The topographic distribution of RGC density in the retinae of both Leach's storm-petrel and Northern fulmar revealed a pronounced horizontal visual streak stretching to the far periphery of the nasal and temporal retina (Figs 2, 3). The six eyes from three adult Leach's storm-petrels had a single central area of increased ganglion cell density – the area centralis – positioned within the visual streak. Retinal thickening was visible even in the retinal wholemounts, but a foveal pit was absent, both in the retinal wholemounts and in cross-sections (Fig. 4A). The six eyes from six Northern fulmars that we examined had a single central fovea (Figs 3, 4C). Here a retinal indentation is clearly indicated where RGCs and cells of the inner nuclear layer were partially displaced to the sides. This clear indicator of a fovea was visible in the retinal wholemounts (Fig. 5) and was also confirmed in the retinal cross-sections (Fig. 4C). Each fovea was positioned within the visual streak, close to the dorsal tip of the pecten. The size and depth of the fovea varied between the specimens (Fig. 5). Two wholemount specimens of the Northern fulmar had the peripheral sides damaged, therefore we present only four RGC maps.

In both species, neurons within the RGC layer varied greatly in size and in shape in the peripheral retina, but were more uniform within the visual streak. Cells were situated in a single layer in the area centralis of Leach's storm-petrel, but were positioned in two or three layers in and around the fovea of the Northern fulmar. Because cells were not organized in ordered stacks, counting and identifying cells was easily achievable by focusing through the layers.

Schematic eye

Gullstrand's simplified schematic eye model yielded an anterior focal length (or *PND*) of 5.4±0.2 mm (mean±s.d.; 3 birds, 3 eyes: 5.1, 5.4 and 5.5 mm; Table 1) for Leach's storm-petrel, which was about half of what we calculated for the Northern fulmar (11.1±0.6 mm; 4 birds, 5 eyes). Likewise, the axial length was 8.2±0.3 mm (3 birds, 3 eyes: 7.9, 8.1 and 8.8 mm; Leach's storm-petrel) and 16.1±0.4 mm (4 birds, 5 eyes; Northern fulmar). The mean maximum entrance pupil diameter was 3.1±0.2 mm (6 birds, 6 eyes) for the Leach's storm-petrel and 7.9±1.5 (3 birds, 3 eyes: 6.2, 8.6 and 8.9 mm) for the Northern fulmar. This gave minimum F-numbers of 1.74 for the Leach's storm-petrel and 1.41 for the Northern fulmar.

Retinal ganglion cell density and spatial resolving power

The RGC densities in the ganglion cell layer varied from 500 - 1900 cells mm^{-2} in the periphery to 18200 - 22700 cells mm^{-2} in the area centralis of the Leach's storm-petrels we examined (3 birds, 6 eyes; Table 1). In the Northern fulmar retinae, RGC densities ranged from 1100 - 1500 cells mm^{-2} in the periphery to 19200 - 25200 cells mm^{-2} in the foveal region (6 birds, 6 eyes). In some fulmar

foveae, RGCs were partly displaced from the centre, thus the highest value represents the peak cell density in or next to the centre of the fovea. Based on the peak RGC density the maximum spatial resolution (Eqn1), ranged from 6.8 to 7.6 cyc deg^{-1} (7.1±0.3; mean±s.d.; 3 birds, 6 eyes) in the Leach's storm-petrel, and from 14.4 to 16.6 cyc deg^{-1} (15.5±0.8; 6 birds, 6 eyes) in the Northern fulmar.

Cone oil droplets in the area centralis of the Leach's storm-petrel and in the fovea of the Northern fulmar were positioned in a dense layer (Fig. 4). The mean oil droplet diameter was 2.6±0.3 (mean±s.d.; 2 birds, 2 eyes, 440 cells) in the Leach's storm-petrel area centralis, and 2.5±0.3 (2 birds, 2 eyes, 214 cells) in the Northern fulmar fovea. Maximum spatial resolution based on oil droplet diameter (Eqn 2), was 21.3 cyc deg^{-1} in the Leach's storm-petrel and and 45.8 cyc deg^{-1} in the Northern fulmar (Table 1).

Optical sensitivity

In the area centralis of Leach's storm-petrel, the length of the rod outer segments was 21.7±1.9 μm (mean±s.d.; 2 birds, 2 eyes, 156 cells; Table 1). The rod outer segment diameter was 1.8±0.3 μm (2 birds, 2 eyes, 274 cells). In the Northern fulmar there were no rods directly under the foveal pit, but rods in the perifoveal region were 23.0±1.9 μm (1 bird, 1 eye, 104 cells) in length and 2.1±0.3 μm (2 birds, 2 eyes, 248 cells) in diameter. These parameters yielded an optical sensitivity of 0.22 $\mu m^2 \cdot sr$ for the rods of the Leach's storm-petrel and 0.48 $\mu m^2 \cdot sr$ for the rods of the Northern fulmar. Optical sensitivity values presented here refer to single rod photoreceptors, but we could not determine the degree of spatial summation from this analysis.

Discussion

Spatial resolution

Based on the evidence for correlated trait evolution between the life history and sensory foraging strategies of the two procellariiform species, we predicted that the burrow-nesting, highly olfactory Leach's storm-petrel should have lower spatial resolution compared to the surface-nesting, presumably more visual Northern fulmar. The peak RGC densities and oil droplet diameters found in the Leach's storm-petrel and the Northern fulmar fall within a similar range (Table 1). The posterior nodal distance (PND), however, was two times shorter in the Leach's storm-petrel than in the Northern fulmar, and, thus, is the main factor contributing to the two-fold difference in spatial resolution, if resolution is estimated based on the same retinal cells in both species. However, in the retinae of the Northern fulmar, but not of the Leach's storm-petrel, we found a central fovea (Fig. 4). As we previously addressed, in species with a fovea, photoreceptor density limits spatial resolution because of a high convergence ratio between photoreceptors and RGCs (Oehme, 1964), but in species without a fovea, RGCs limit spatial resolution, because several photoreceptors converge their signals onto one RGC. Thus using photoreceptor density in a species without a fovea would likely result in an overestimate of visual acuity. For these reasons, we conservatively used peak RGC density in the area centralis of the Leach's storm-petrel and photoreceptor density in the fovea of the Northern fulmar to estimate maximum spatial resolution for these species. However, since we also found rods in the area centralis of the Leach's storm-petrel, this may indicate the presence of rod-specific ganglion cells; thus the true anatomical spatial resolving power of this species might be lower.

We found that Leach's storm-petrel has around six times lower spatial resolution than the Northern fulmar (Leach's storm-petrel: 7.1 cyc deg^{-1}; Northern fulmar: 45.8 cyc deg^{-1}). The only other procellariiform seabird for which comparable data exist is the Manx shearwater (*Puffinus puffinus*). The posterior nodal distance of the Manx shearwater is 6.5 mm (Martin and Brooke, 1991). Its retina has a peak RGC density of 21500 cells mm^{-2}, but has no fovea (Hayes and Brooke, 1990). The anatomical spatial resolution of the Manx shearwater is, therefore, 8.9 cyc deg^{-1}, and is similar to the resolution of the Leach's storm-petrel.

We can also compare our study species to other more highly studied non-procellariiform species. The Japanese quail (*Coturnix japonica*; PND=5.6 mm), a galliform species, has a similar PND to the Leach's storm petrel and also lacks a fovea. However, Japanese quail also has a much higher peak RGC density (35115 cells mm^{-2}) than the Leach's storm-petrel, and, therefore, higher spatial resolution (9.7 cyc deg^{-1}; Lisney et al., 2012b). The common kestrel (PND=10.2 mm), a falconiform species, has a similar PND to the Northern fulmar and also has a fovea. However, the common kestrel has much higher cone density in the central fovea (385813 cells mm^{-2}), and therefore higher

anatomical spatial resolution (59.1 cyc deg^{-1}; Oehme, 1964). These comparisons suggest that neither the Leach's storm-petrel nor the Northern fulmar has maximized retinal cell densities to achieve the spatial resolution possible considering eye size alone. However, among the procellariiforms that have been studied, the presence of a fovea is so far only noted in surface-nesting species (the Northern fulmar (this study), the shy albatross (*Thalassarche cauta;* formerly known as *Diomedea cauta*, see O'Day, 1940) and the Southern giant petrel (*Macronectes giganteus*; O'Day, 1940), but not in burrow nesting species (Leach's storm-petrel (this study) and Manx shearwater (Hayes and Brooke, 1990)). These results suggest that surface nesters may be adapted to have higher visual acuity than burrow nesting species.

Northern fulmars have about six times greater spatial resolution than the Leach's storm-petrel suggesting that, under the same visual conditions, Northern fulmars can resolve distant objects from about six times greater distance. However, anatomical spatial resolution should be considered as the maximum theoretical limit achievable only in bright light and when viewing highly contrasting objects. It is well known that visual acuity deteriorates drastically as ambient light level and contrast of the object to the background decreases (Reymond, 1985; Lind et al., 2012).

Assessing differences in visual ability in real world scenarios

What does this information tell us about how visual ability compares between Leach's storm-petrels and Northern fulmars in the real world environment where the birds are foraging? Here we presented a theoretical maximum of the anatomical spatial resolution; however, contrast sensitivity must also be considered in judging how spatial resolution translates to real world problems. Contrast sensitivity describes the ability to detect brightness differences between an object and its background and cannot be evaluated using anatomical measures. There are many factors in a natural environment that will impact detectable contrast for a bird flying above the ocean. Sun direction, reflections from the water surface, moving clouds, rain and fog all will have an effect on the contrast an object of interest presents against the background. Depending on the direction of view, even the same object may be visible or invisible for two identical observers.

In the few species that have been investigated with behavioural methods (e.g. barn owl (*Tyto alba*), wedge-tailed eagle, chicken, pigeon (*Columba livia*), parrots), birds have been shown to have lower contrast sensitivity compared to humans and some other mammals (summary in Lind et al., 2012). The minimum contrast birds can detect ranges from 7 to 14% (Reymond and Wolfe, 1981; Ghim and Hodos, 2006; Harmening et al., 2009; Jarvis et al., 2009; Lind et al., 2012). By way of comparison, humans can detect contrast differences as low as 0.6% (De Valois and Morgan, 1974), but spatial resolution decreases more than eleven times as contrast goes down from 100% to 0.6%. In birds, resolution decreases more than six times as contrast goes down from 100% to 7-14% depending on the species (Reymond and Wolfe, 1981; Ghim and Hodos, 2006; Harmening et al.,

2009; Jarvis et al., 2009; Lind et al., 2012). If we assume a similar decrease in spatial resolution for our study species as in other birds, then Leach's storm-petrels would be able to detect lowest contrast with a spatial resolution of 1.1 cyc deg^{-1}, whereas Northern fulmars with a resolution of 7.2 cyc deg^{-1}. This conservative approximation of possible spatial resolution when the contrast of an object to the background is low allows us to calculate possible sighting distances for food items and other objects on the ocean.

The diet of both species includes crustaceans, fish and cephalopods. Both species are known to take prey by surface-seizing, but can also snatch it by dipping (Brooke, 2004), which means that they can detect prey just beneath the water surface in flight. Pennycuick (1982) reported that Wilson's storm-petrels (*Oceanites oceanicus*) rarely fly higher than two meters above the water, and Haney et al. (1992) suggested that 8-13 meters is the upper limit for the search flight in several larger procellariiform species. Therefore, in a conservative scenario, if we assume that a Leach's storm-petrel is flying at a height of 2 meters, then, with a spatial resolution of 1.1 cyc deg^{-1}, the smallest low-contrast object it could see is 16 mm in diameter, while the smallest, high-contrast object (thus, with a resolution of 7.1 cyc deg^{-1}) would be around 2.5 mm (Eqn 3). If a Northern fulmar is looking down at the water from a height of 8 meters, then with a spatial resolution of 7.2 cyc deg^{-1}, the smallest low-contrast object it could see is 10 mm in diameter while an object with high-contrast (thus, with a resolution of 45.8 cyc deg^{-1}) could be a small as 1.5 mm. Accordingly much smaller prey items could be seized when the birds are nearer to the water's surface, and larger prey could be detected from a longer distance.

In addition to the limitations of resolution and contrast sensitivity, ocean swell and wave height are direct obstacles for spotting and navigating to distant objects at sea. This is especially the case for objects close to the water surface, such as other low flying birds or small boats. The effect of swell and waves on blocking the view is specific in every situation, but apart from that, the geometry of the Earth puts a final limit on the sighting of very distant and even high contrast objects in bright and clear daylight conditions.

On Earth, the distance to the flat horizon can be calculated as a function of the height of the observer's eye above the water ($[3.838 \times (H_{obs})^{0.5}]$; Haney et al., 1992). The object behind the horizon has exactly the same relationship to its horizon ($[3.838 \times (H_{obj})^{0.5}]$). Consequently, the sighting distance between the observer and the object is simply the sum of two. Procellariifom seabirds typically require wind and updraft off waves to maintain flight. Therefore, in an abnormal, but nonetheless theoretically illuminating situation where swell and waves are absent, the theoretical geometrical line of sight between two birds at height of 2 meters would be almost 11 kilometres. For Leach's storm-petrel with a spatial resolution of 1.1 cyc deg^{-1}, the smallest low-contrast object that can be resolved at a distance of 11 km would have to be as large as 87 meters

(Eqn 3). For the Northern fulmar (7.2 cyc deg^{-1}) this object would have to be at least 13 meters in diameter. Clearly, even with the best weather conditions, neither of these species could see another conspecific from such a distance. Thus, the geometry of the Earth can limit sighting distance only of large objects like fishing vessels or high islands. However, due to swell, waves, flight trajectory, and the bird's height above the water, maximum sighting distance would fluctuate and be considerably reduced compared to this theoretical maximum, even on a bright day with clear sky. Thus any estimates for detection distances, especially for objects far from the observer, should be taken with special caution, because, apart from the geometry and direct obstacles to the line of sight, meteorological conditions can impair visibility. Finally, as the light levels drop, contrast sensitivity as well as spatial resolution also rapidly decreases (Lind et al., 2012).

Optical sensitivity

The Leach's storm-petrel and the Northern fulmar have contrasting nesting behaviours and activity patterns at the colony. Leach's storm-petrels have their nests in deep burrows or crevices on rocky slopes, in grassland, or between trees (Brooke, 2004). They enter and leave their burrows strictly under the cover of darkness and it has been suggested that they avoid coming to the colony on moonlit nights in order to avoid predation (Watanuki, 1986). Northern fulmars breed on cliffs and visit the nest both during day and night (Danielsen, 2011). We expected, therefore, that Leach's storm-petrel should have more sensitive eyes (better night vision) than the Northern fulmar.

A large pupil diameter usually suggests a sensitive eye. However, even a small eye, with a small pupil, can achieve a bright retinal image, because sensitivity to extended visual scenes (as compared to point sources of light) is inversely proportional to the F-number (Warrant and Nilsson, 1998), which is the ratio between the focal length and pupil diameter. Thus, even though the Leach's storm-petrel has less than half the pupil diameter of the Northern fulmar, both species have similar F-numbers (1.74 and 1.41 respectively). These values fall between the F-numbers of a pigeon (1.98) and a Tawny owl (*Strix aluco*; 1.3), and are lower than F-numbers reported in humans (2.1) (Martin, 1983).

At the level of the retina, the rods of the Leach's storm-petrel and the Northern fulmar have similar dimensions (21.7 and 23.0 μm in length, 1.8 and 2.1 μm in width, respectively) and therefore similar optical sensitivity (0.22 and 0.48 $\mu m^2 \cdot sr$, respectively). Because the dimmest starlight is thousand times darker than the brightest moonlight, differences in optical sensitivity are meaningful only on the level of orders of magnitude. With this in mind, optical sensitivity at the level of the single rod photoreceptor is very similar in the two species. If spatial pooling (the neuronal integration of signals from many photoreceptors) were adjusted for the same spatial resolution in both species, the Northern fulmar would have an optical advantage due to the larger pupil diameter. However, as the level of spatial pooling in these species remains unknown, the question as to

whether the Leach's storm-petrels or the Northern fulmars have sharper vision in dim light remains to be answered. Recent observations suggest that Northern fulmars leave nesting colonies during sunset and return during sunrise, suggesting that they are highly adapted for navigating in dim light to and from the colony (Danielsen, 2011).

Retinal ganglion cell topography

Both Leach's storm-petrel and the Northern fulmar have horizontal visual streaks reaching to the far periphery of the nasal and temporal retina. The visual streaks of both species were well pronounced and similar to those found in the Manx shearwater, soft-plumaged petrel (*Pterodroma mollis*) and common diving-petrel (*Pelecanoides urinatrix*) (Hayes and Brooke, 1990). This retinal adaptation allows birds to observe a large part of the horizon without the need to move the eyes or the head and is presumed to be advantageous for animals living in open habitats (Hughes, 1977). Our results are in agreement with the "terrain theory" proposed by Hughes (1977). However, Hayes and Brooke (1990) have found that the Kerguelen petrel (*Aphrodroma brevirostris*) lacks a visual streak, but has a concentric distribution of the RGC density lines. Therefore, not only the "openness" of the habitat, but also other factors like foraging strategy, prey capture technique, activity pattern and phylogenetic relatedness might influence the evolution of the RGC distribution in the retina (Hayes and Brooke, 1990; Lisney et al., 2012a, 2012b, 2013).

Concluding remarks

Our anatomical results support the hypothesis that differences in vision likely contribute to the sensory ecology of foraging and are also linked to life history nesting strategies (Van Buskirk and Nevitt, 2008). We show that Leach's storm-petrel, a cryptic burrow-nesting species that tracks odour cues such as DMS as part of its foraging strategy, has less acute vision than the Northern fulmar, a larger, presumably more visual forager that nests in the open. The differences we report in visual acuity can be attributed, in part, to differences in eye size correlated to body size (Brooke et al., 1999)). However, we also show distinct anatomical differences in retinal adaptations: the Leach's storm-petrel has an area centralis, while the Northern fulmar has a distinct fovea. In contrast to our second expectation, that Leach's storm-petrels, which are strictly nocturnal at a colony, should have higher sensitivity (better night vision) than Northern fulmars, we found similar optical sensitivity in both species. Finally, the eyes of both species have a visual streak that allows them to look at large parts of the visual field with higher resolution without a need to move the eyes or the head, and to potentially observe large foraging aggregations, shipping vessels or islands on the horizon.

Acknowledgements

We would like to thank Lee and Carline Adams, Dave Shutler (Acadia university, Wolfville), Russell Easy (Dalhousie University, Halifax), Brian Hoover (UC Davis, Davis), Maria Dam (Umhvørvisstovan, Environment Agency, Tórshavn), Niels Pauli Djurhuus, Eirikur Danielsen, Carina Rasmussen, Eva Landgren and Ola Gustafsson for all types of practical and scientific support during different stages of the project. We thank João Paulo Coimbra for useful comments on earlier versions of the manuscript.

Competing interests

The authors declare no competing or financial interests.

Author contributions

M.M., G.A.N. and A.K. had the original idea and planned the project. M.M., G.A.N., J.D. and A.K. did the fieldwork and collected the samples. M.M. did the sample analysis in the laboratory. M.M., G.A.N., J.D. and A.K. analysed the data and wrote the paper.

Funding

M.M and A.K were funded by the Crafoord Foundation, the Royal Physiographic Society in Lund, the Knut and Alice Wallenberg Foundation, the Swedish Research Council (621-2009-5683, 2012-2212); G.A.N was funded by the National Science Foundation Division of Integrative Organismal Systems (1258828) and Division of Polar Programs (1142084).

References

Boire, D., Dufour, J.-S., Theoret, H. and Ptito, M. (2001). Quantitative analysis of the retinal ganglion cell layer in the ostrich, *Struthio camelus*. *Brain, Behav. Evol*. **58**, 343-355.

Brooke, M. (2004). *Albatrosses and Petrels across the World*. Oxford, UK: Oxford University Press.

Chen, Y. and Naito, J. (1999). A quantitative analysis of cells in the ganglion cell layer of the chick retina. *Brain, Behav. Evol*. **53**, 75-86.

Coimbra, J.P., Collin, S.P. and Hart, N.S. (2015). Variations in retinal photoreceptor topography and the organization of the rod-free zone reflect behavioral diversity in Australian passerines. *J. Comp. Neurol*. **523**, 1073-1094.

Coimbra, J.P., Nolan, P.M., Collin, S.P. and Hart, N.S. (2012). Retinal ganglion cell topography and spatial resolving power in penguins. *Brain, Behav. Evol*. **80**, 254-268.

Collin, S.P. and Pettigrew, J.D. (1988). Retinal ganglion cell topography in teleosts: a comparison between Nissl-stained material and retrograde labelling from the optic nerve. *J. Comp. Neurol.* **276**, 412-422.

Danielsen, J. (2011). Diurnal activity patterns suggest nocturnal foraging in Northern fulmar (*Fulmarus glacialis*). *Fróðskaparrit* **59**, 113-120.

De Valois, R.L. and Morgan, H. (1974). Psychophysical studies of monkey vision-III. Spatial luminance contrast sensitivity tests of macaque and human observers. *Vision Res.* **14**, 75-81.

Dolan, T. and Fernández-Juricic, E. (2010). Retinal ganglion cell topography of five species of ground-foraging birds. *Brain, Behav. Evol.* **75**, 111-121.

Ehrlich, D. (1981). Regional specialization of the chick retina as revealed by the size and density of neurons in the ganglion cell layer. *J. Comp. Neurol.* **195**, 643-657.

Ghim, M.M. and Hodos, W. (2006). Spatial contrast sensitivity in birds. *J. Comp. Physiol. A* **192**, 523-534.

Gundersen, H.J.G. (1977). Notes on the estimation of the numerical density of arbitrary profiles: the edge effect. *J. Microsc*. **111**, 219-223.

Haney, J.C., Fristrup, M.F. and Lee, D.S. (1992). Geometry of visual recruitment by seabirds to ephemeral foraging flocks. *Ornis Scand.* **23**, 49-62.

Harmening, W.M., Nikolay, P., Orlowski, J. and Wagner, H. (2009). Spatial contrast sensitivity and grating acuity of barn owls. *J. Vision* **9**, 1-12.

Harmening, W.M., Vobig, M.A., Walter, P. and Wagner, H. (2007). Ocular aberrations in barn owl eyes. *Vision Res.* **47**, 2934-2942.

Hayes, B.P. and Brooke, M.D. (1990). Retinal ganglion cell distribution and behaviour in procellariiform seabirds. *Vision Res*. **30**, 1277-1289.

Hughes, A. (1977). The topography of vision in mammals of contrasting life style: comparative optics and retinal organization. In *Handbook of sensory physiology, vol. VII/5* (ed. F. Crescitelli), pp. 613-756. Berlin: Springer.

Jarvis, J.R., Abeyesinghe, S.M., McMahon, C.E. and Wathes, C.M. (2009). Measuring and modelling the spatial contrast sensitivity of the chicken (*Gallus g. domesticus*). *Vision Res.* **49**, 1448-1454.

Kram,Y.A., Mantey, S. and Corbo, J.C. (2010). Avian cone photoreceptros tile the retina as five independent, self-organizing mosaics. *PLoS One,* 5(2): e8992. doi:10.1371/journal.pone.0008992

Land, M.F. and Nilsson, D-E. (2012). *Animal eyes*. Oxford, UK: Oxford University Press.

Lind, O. and Kelber, A. (2009). The intensity threshold of colour vision in two species of parrot. *J. Exp. Biol.* **212**, 3693-3699.

Lind, O., Sunesson, T., Mitkus, M. and Kelber, A. (2012). Luminance-dependance of spatial vision in budgerigars (*Melopsittacus undulatus*) and Bourke's parrots (*Neopsephotus bourkii*). *J. Comp. Physiol. A* **198**, 69-77.

Lisney, T.J., Iwaniuk, A.N., Bandet, M.V. and Wylie, D.W. (2012a) Eye shape and retinal topography in owls (Aves: Strigiformes). *Brain, Behav. Evol.* **79**, 218–236.

Lisney, T.J., Iwaniuk, A.N., Kolominsky, J., Bandet, M.V., Corfield, J.R. and Wylie, D.W. (2012b). Interspecific variation in eye shape and retinal topography in seven species of galliform bird (Aves: Galliformes: Phasianidae). *J. Comp. Physiol. A* **198**, 717-731.

Lisney, T.J., Stecyk, K., Kolominsky, J., Schmidt, B.K., Corfield, J.R., Iwaniuk, A.N. and Wylie, D.R. (2013). Ecomorphology of eye shape and retinal topography in waterfowl (Aves: Anseriformes: Anatidae) with different foraging modes. *J. Comp. Physiol. A* **199**, 385-402.

Maier, F.M., Howland, H.C., Ohlendorft, A., Wahl, S. and Schaeffel, F. (2015). Lack of oblique astigmatism in the chicken eye. *Vision Res.* **109**, 68-76.

Martin, G.R. (1983). Schematic eye models in vertebrates. In *Progress in Sensory Physiology, Vol 4* (eds H. Autrum, D. Ottoson, E.R. Perl, R.F. Schmidt, H. Shimazu, and W.D. Willis), pp. 43-81. Berlin: Springer-Verlag.

Martin, G.R. and Brooke, M.D.L. (1991). The eye of a Procellariiform seabird, the Manx shearwater, *Puffinus puffinus*: visual fields and optical structure. *Brain, Behav. Evol*. **37**, 65-78.

Mitkus, M., Chaib, S., Lind, O. and Kelber, A. (2014). Retinal ganglion cell topography and spatial resolution of two parrot species: budgerigar (*Melopsittacus undulatus*) and Bourke's parrot (*Neopsephotus bourkii*). *J. Comp. Physiol. A* **200**, 371-384.

Moore, B.A., Doppler, M., Young, E.J. and Fernández-Juricic, E. (2013). Interspecific differences in the visual system and scanning behavior of three forest passerines that from heterospecific flocks. *J. Comp. Physiol. A* **199**, 263-277.

Nevitt, G.A. (2008). Sensory ecology on the high seas: The odor world of the procellariiform seabirds. *J. Exp. Biol.* **211**, 1706-1713.

Nevitt, G.A. (2011). The neuroecology of dimethyl sulphide: a global-climate regulator turned marine infochemical. *Integr. Comp. Biol.* **51**, 819-825.

Nevitt, G.A. and Bonadonna, F. (2005). Sensitivity to dimethyl sulphide suggests a mechanism for olfactory navigation by seabirds. *Biol. Lett.* **1**, 303-305.

Nevitt, G.A., Reid, K. and Trathan, P. (2004). Testing olfactory foraging strategies in an Antarctic seabird assemblage. *J. Exp. Biol.* **207**, 3537-3544.

Nevitt, G.A., Veit, R.R. and Kareiva, P. (1995). Dimethyl sulphide as a foraging cue for Antarctic Procellariifom seabirds. *Nature*, **376**, 680-682.

O'Day, K. (1940). The fundus and fovea centralis of the albatross (*Diomedea cauta cauta* Gould). *Brit. J. Ophthal.* **24**, 201-207.

Oehme, H. (1964). Vergleichende Untersuchungen an Greifvogelaugen. *Z. Morph. Ökol. Tiere* **53**, 618-635.

Pennycuick, C.J. (1982). The flight of petrels and albatrosses (Procellariiformes), observed in South Georgia and its vicinity. *Phil. Trans. R. Soc. B* **300**, 75-106.

Pettigrew, J.D., Dreher, B., Hopkins, C.S., McCall, M.J. and Brown, M. (1988). Peak density and distribution of ganglion cells in the retinae of microchiropteran bats: implications for visual acuity. *Brain, Behav. Evol.* **32**, 39-56.

Rasband, W.S. (1997–2012). Image J. US National Institutes of Health, Bethesda. http://imagej.nih.gov/ij/

Reymond, L. (1985). Spatial visual acuity of the eagle, *Aquila audax*: a behavioural, optical and anatomical investigation. *Vision Res.* **25**, 1477-1491.

Reymond, L. (1987). Spatial visual acuity of the falcon, *Falco berigora*: a behavioural, optical and anatomical investigation. *Vision Res.* **27**, 1859-1874.

Reymond, L. and Wolfe, J. (1981). Behavioural determination of the contrast sensitivity function of the eagle *Aquila audax*. *Vision Res.* **21**, 263–271.

Savoca, M.S. and Nevitt, G.A. (2014). Evidence that dimethyl sulfide facilitates a tritrophic mutualism between marine primary producers and top predators. *PNAS*, **111**, 4157-4161.

Snyder, A.W. and Miller, H.M. (1977). Photoreceptor diameter and spacing for highest resolving power. *J. Opt. Soc. Am.* **67**, 696–698.

Stavenga, D.G. and Wilts, B.D. (2014). Oil droplets of bird eyes: microlenses acting as spectral filters. *Phil. Trans. R. Soc. B* **369**, 20130041.

Stone, J. (1981). *The wholemount book. A guide to preparation and analysis of retinal wholemounts*. Sydney: Maitland Publications Pty. Ltd.

Van Buskirk, R.W. and Nevitt, G.A. (2008). The influence of developmental environment on the evolution of olfactory foraging behaviour in procellariiform seabirds. *J. Evol. Biol.* **21**, 67-76.

Warrant, E.J. and Nilsson, D-E. (1998). Absorption of white light in photoreceptors. *Vision Res.* **38**, 195-207.

Wässle, H., Grünert, U., Röhrenbeck, J. and Boycott, B.B. (1990). Retinal ganglion cell density and cortical magnification factor in the primate. *Vision Res.* **30**, 1897–1911.

Watanuki, Y. (1986). Moonlight avoidance behaviour in Leach's storm-petrels as a defence against slaty-backed gulls. *The Auk* **103**, 14-22.

Williams, D.R. and Coletta, N.J. (1987). Cone spacing and the visual resolution limit. *J. Opt. Soc. Am.* **4**, 1514–1523.

Figures

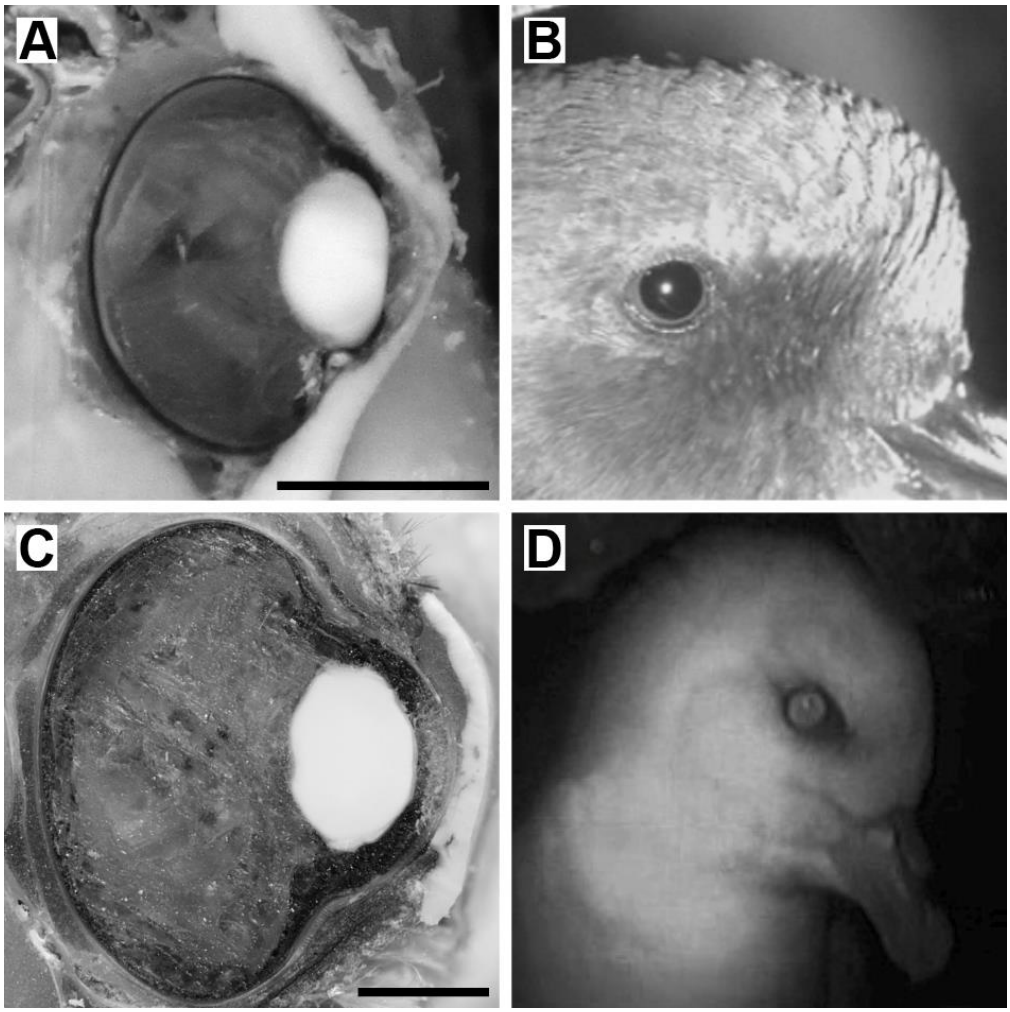

Fig. 1. Eyes of the Leach's storm-petrel (A, B) and Northern fulmar (C, D). (A) and (C) - examples of cryo-sectioned eyes used to calculate posterior nodal distance, (B) and (D) - video frames extracted from the infrared camcorder footage used to measure maximum pupil diameter. Scale bars - 5 mm in (A) and (C).

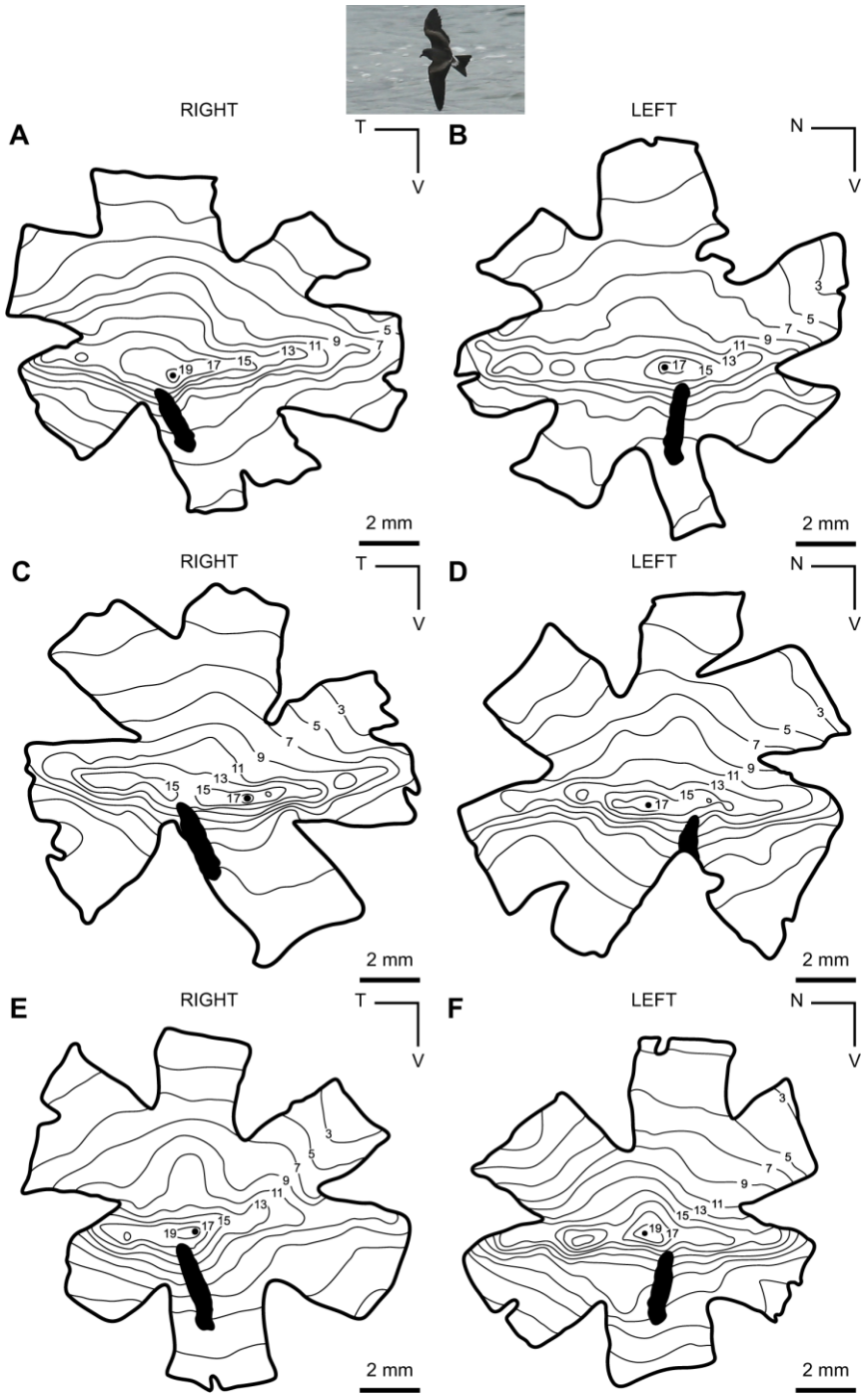

Fig. 2. Retinal ganglion cell topography in Leach's storm-petrel. A and B, C and D, E and F are the left and right eyes of the same individuals. Numbers represent ×1000 cells mm^{-2}. Black oblique bars indicate the position of the pecten and the optic nerve head, the region where there are no RGC present. Black dots indicate the regions of peak RGC density: (A) – 19141; (B) – 18256; (C) – 18172; (D) - 19294; (E) – 20615; (F) – 22674 cells mm^{-2}. N - nasal, V - ventral, T – temporal. Insert picture courtesy: Seabamirum / Wikimedia Commons / Public Domain

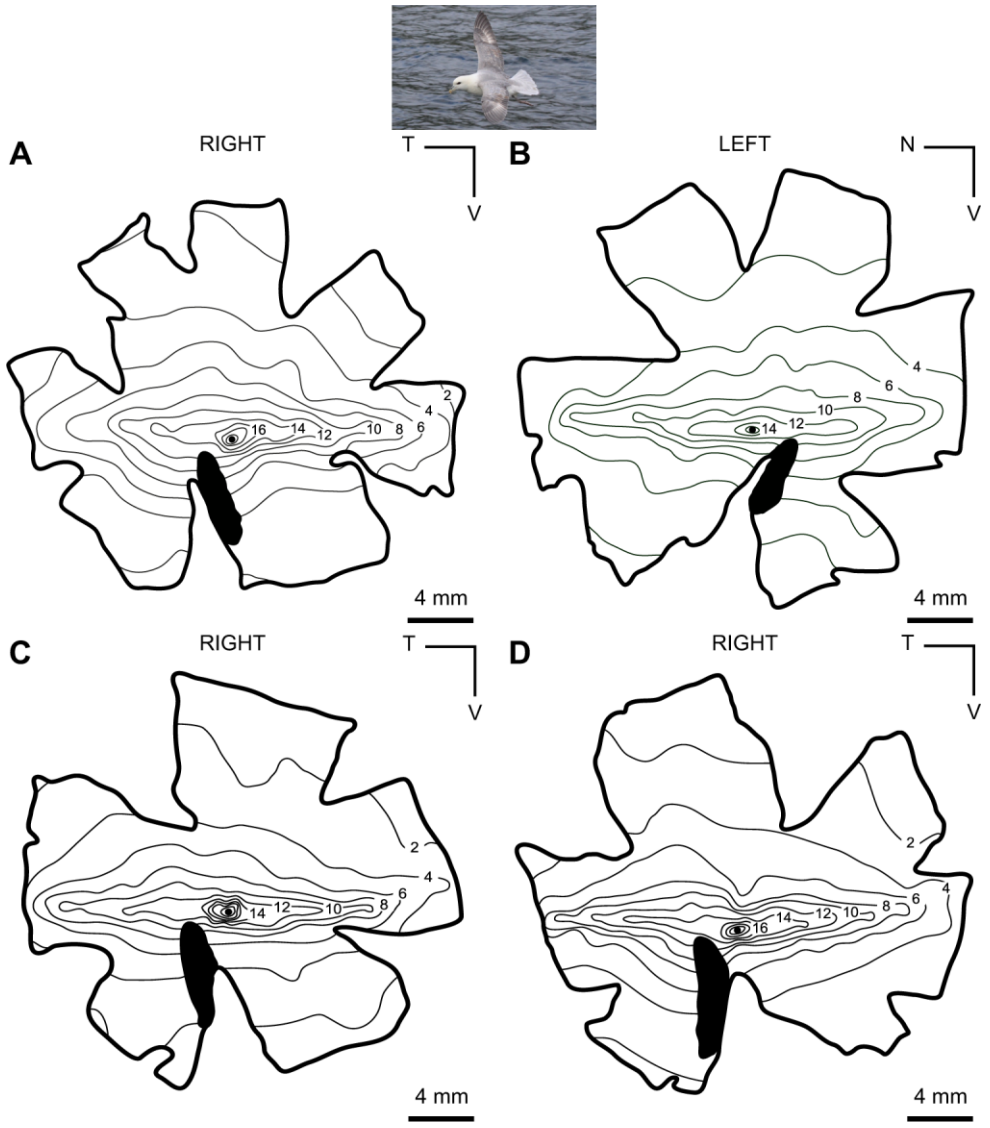

Fig. 3. Retinal ganglion cell topography in the Northern fulmar. Numbers represent ×1000 cells mm^{-2}. Black oblique bars indicate the position of the pecten and the optic nerve head, the region where there are no RGCs present. Black dots indicate the regions of the central fovea. The peak RGC density was: (A) – 21678; (B) – 19222; (C) – 23607; (D) –20214 cells mm^{-2}. N - nasal, V - ventral, T - temporal. Insert picture courtesy: Mindaugas Mitkus

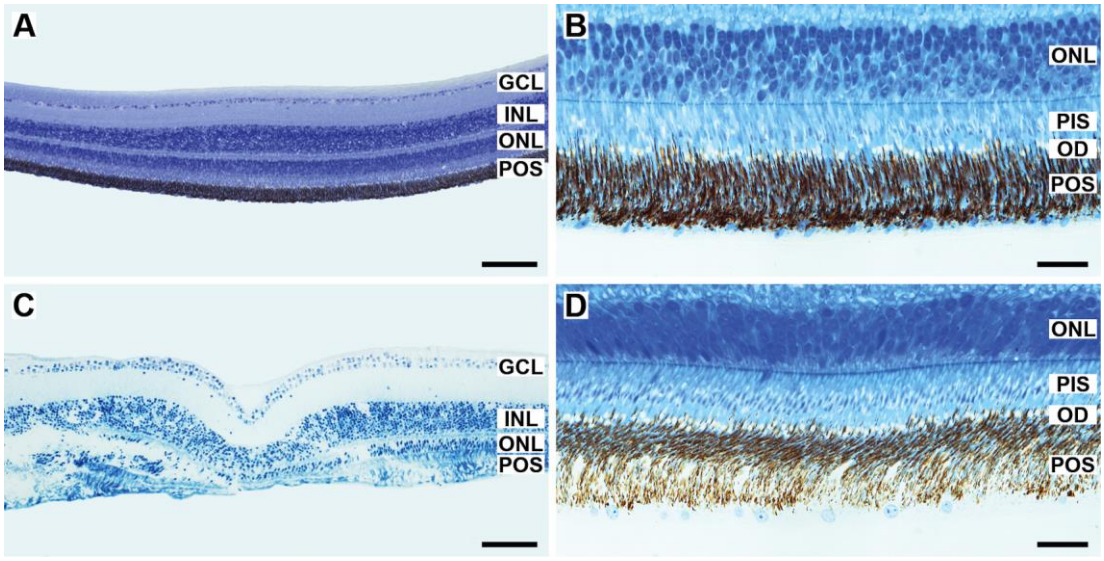

Fig. 4. Retinal cross-section view through the area centralis of the Leach's storm-petrel (A, B) and central fovea of the Northern fulmar (C, D). GCL - ganglion cell layer, INL - inner nuclear layer, ONL - outer nuclear layer, POS - photoreceptor outer segments. Scale bar - 100 μm in (A) and (C); 20 μm in (B) and (D).

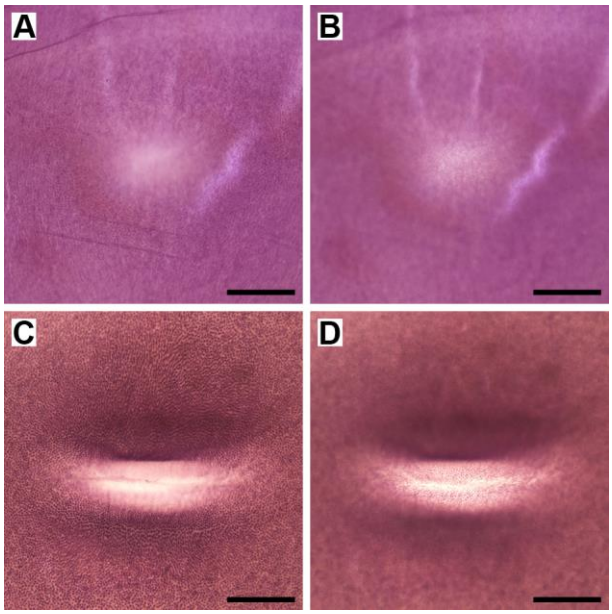

Fig. 5. Wholemount view of the Northern fulmar central fovea. (A) and (B) illustrates round fovea from one individual, (C) and (D) illustrates elongated fovea from another individual. Pictures (A) and (C) have focus on the foveal rim, (B) and (D) – on the foveal pit. Scale bars - 200 μm.

Table

Table 1. Optical and anatomical parameters for the eyes of the Leach's storm-petrel and the Northern fulmar.

	Units	Leach's storm-petrel	Northern fulmar
Average peak neuronal (ganglion + displaced amacrine) cell density	cells mm^{-2}	19692±1708 (18172-22674) (N=3; n=6)	22123±2221 (19221-25254) (N=6; n=6)
Spatial resolution (based on neuronal cells)	cyc deg^{-1}	7.1±0.3 (6.8-7.6) (N=3; n=6)	15.5±0.8 (14.4-16.5) (N=6; n=6)
Oil droplet diameter (area centralis or fovea)	μm	2.6±0.3 (N=2; n=2; C=440)	2.5±0.3 (N=2; n=2; C=214)
Spatial resolution (based on oil droplet diameter)	cyc deg^{-1}	21.3 (20.9-21.8) (N=2; n=2)	45.8 (43.0-48.6) (N=2; n=2)
Axial length	mm	8.2±0.3 (N=3; n=3)	16.2±0.5 (N=4; n=5)
Posterior nodal distance (PND)	mm	5.4±0.2 (N=3; n=3)	11.1±0.6 (N=4; n=5)
Retinal magnification factor	mm deg^{-1}	0.094	0.194
Max entrance pupil diameter	mm	3.1±0.2 (N=6; n=6)	7.9±1.5 (N=3; n=3)
F-number	n.a.	1.74	1.41
Retinal image brightness	n.a.	3.03	1.97
Rod outer segment length (area centralis and perifovea)	μm	21.7±1.9 (N=2; n=2; C=156)	23.0±1.9 (N=1; n=1; C=104)
Rod outer segment diameter (area centralis and perifovea)	μm	1.8±0.3 (N=2; n=2; C=274)	2.1±0.3 (N=2; n=2; C=248)
Optical sensitivity of rods (area centralis and perifovea)	$\mu m^2 \cdot sr$	0.22	0.48

Values are mean±s.d. where applicable. The range is indicated in parentheses.

N – number of individuals; n – number of eyes; C – number of cells measured; n.a. – not applicable